Title

Delayed afterdepolarizations generate both triggers and a vulnerable substrate promoting reentry in cardiac tissue

Journal

Heart Rhythm, 12(10)

ISSN

1547-5271

Authors

Liu, MB
De Lange, E
Garfinkel, A
et al.

Publication Date

2015-10-01

DOI

10.1016/j.hrthm.2015.06.019

Peer reviewed

Delayed afterdepolarizations generate both triggers and a vulnerable substrate promoting reentry in cardiac tissue

Michael B. Liu, MS,[*†] Enno de Lange, PhD,[*‡] Alan Garfinkel, PhD,[*†§] James N. Weiss, MD,[*†§¶] Zhilin Qu, PhD[*†]

From the [*]UCLA Cardiovascular Research Laboratory, [†]Department of Medicine (Cardiology), David Geffen School of Medicine, University of California, Los Angeles, California, [‡]Department of Knowledge Engineering, Maastricht University, Maastricht, The Netherlands, [§]Department of Integrative Biology and Physiology, University of California, Los Angeles, California, and [¶]Department of Physiology, David Geffen School of Medicine, University of California, Los Angeles, California.

BACKGROUND Delayed afterdepolarizations (DADs) have been well characterized as arrhythmia triggers, but their role in generating a tissue substrate vulnerable to reentry is not well understood.

OBJECTIVE The purpose of this study was to test the hypothesis that random DADs can self-organize to generate both an arrhythmia trigger and a vulnerable substrate simultaneously in cardiac tissue as a result of gap junction coupling.

METHODS Computer simulations in 1-dimensional cable and 2-dimensional tissue models were performed. The cellular DAD amplitude was varied by changing the strength of sarcoplasmic reticulum calcium release. Random DAD latency and amplitude in different cells were simulated using gaussian distributions.

RESULTS Depending on the strength of spontaneous sarcoplasmic reticulum calcium release and other conditions, random DADs in cardiac tissue resulted in the following behaviors: (1) triggered activity (TA); (2) a vulnerable tissue substrate causing unidirectional conduction block and reentry by inactivating sodium channels; (3) both triggers and a vulnerable substrate simultaneously by generating TA in regions next to regions with subthreshold DADs susceptible to unidirectional conduction block and reentry. The probability of the latter 2 behaviors was enhanced by reduced sodium channel availability, reduced gap junction coupling, increased tissue heterogeneity, and less synchronous DAD latency.

CONCLUSION DADs can self-organize in tissue to generate arrhythmia triggers, a vulnerable tissue substrate, and both simultaneously. Reduced sodium channel availability and gap junction coupling potentiate this mechanism of arrhythmias, which are relevant to a variety of heart disease conditions.

KEYWORDS Delayed afterdepolarization; Conduction block; Reentry; Arrhythmia; Computer simulation

ABBREVIATIONS **1D** = 1-dimensional; **2D** = 2-dimensional; **AP** = action potential; **Ca** = calcium; **CaMKII** = Ca/calmodulin-dependent protein kinase II; **DAD** = delayed afterdepolarization; **Na** = sodium; **PKA** = protein kinase A; **PKC** = protein kinase C; **PVC** = premature ventricular complex; **SR** = sarcoplasmic reticulum; **TA** = triggered activity

(Heart Rhythm 2015;12:2115–2124)

Introduction

Delayed afterdepolarizations (DADs) are transient depolarizations in the diastolic phase following an action potential (AP) that have been linked to arrhythmogenesis in cardiac diseases.[1–3] Experimental studies have revealed that the primary cause of DADs is spontaneous sarcoplasmic reticulum (SR) calcium (Ca) release, which activates Ca-sensitive inward currents such as the sodium–calcium (Na–Ca) exchange current to depolarize diastolic membrane potential. Ca waves are promoted under Ca overload conditions in normal myocytes[4,5] or under diseased conditions, such as heart failure,[6–8] ischemia,[9] catecholaminergic polymorphic ventricular tachycardia,[10] and long QT syndromes.[11,12]

The role of DADs in arrhythmogenesis is generally explained as follows. When the amplitude of a DAD is above a certain threshold (termed a *suprathreshold* DAD), it can trigger an AP, called triggered activity (TA), which can cause a premature ventricular complex (PVC) to trigger reentrant or focal arrhythmias.[3,13] However, not all DADs

Mr. Liu and Dr. de Lange contributed equally to this manuscript. Supported by National Institutes of Health, National Heart, Lung, and Blood Institute Grants P01 HL078931 and R01 HL110791; UCLA MSTP Grant T32 GM008042 to Mr. Liu; the Swiss Foundation for Grants in Biology and Medicine grant PASMP3-127312 to Dr. de Lange; and the Laubisch and Kawata endowments. **Address reprint requests and correspondence:** Dr. Zhilin Qu, Department of Medicine, Division of Cardiology, David Geffen School of Medicine at UCLA, A2-237 CHS, 650 Charles E. Young Drive South, Los Angeles, CA 90095. E-mail address: zqu@mednet.ucla.edu.

are large enough to trigger APs, and the role of these *subthreshold* DADs in arrhythmogenesis is not well understood. It is well known that elevation of resting membrane potential can cause conduction slowing and block.[14] Elevation of the resting membrane potential of a ventricular myocyte will first enhance conduction by moving the potential closer to the Na channel activation threshold, but further elevation will slow conduction due to Na channel inactivation. In an experimental study, Rosen et al[15] showed that impulses occurring during a DAD in a Purkinje fiber did not propagate to the ventricles, whereas earlier or later impulses did, suggesting that DADs can cause conduction block in Purkinje fibers. However, to our knowledge, no other studies have been carried out to investigate the role of subthreshold DADs as causes of conduction block and/or reentry.

The amplitude and latency of diastolic Ca waves tend to vary irregularly from beat to beat as a result of random properties of spontaneous SR Ca release,[5,16,17] which can be further enhanced because of cell-to-cell or regional heterogeneities in Ca cycling properties.[3,18] However, myocytes in cardiac tissue are coupled via gap junctions, which tend to smooth the voltage differences between adjacent cells, synchronizing their depolarizations locally. These 2 competing factors could interact to generate regions of tissue with suprathreshold DADs causing TA bordering on regions with subthreshold DADs susceptible to conduction block, initiating reentry.

Based on this reasoning, we hypothesized that depending on the SR Ca release strength and other conditions, random DADs can self-organize in tissue to cause (1) arrhythmia triggers by generating PVCs; (2) a vulnerable tissue substrate causing unidirectional conduction block of a PVC; and (3) both simultaneously, resulting in initiation of reentry. To test this hypothesis, we performed computer simulations in 1-dimensional (1D) cables and 2-dimensional (2D) tissue models. DADs were simulated by commanded SR Ca releases, similar to DADs induced in experiments by caffeine pulses[19] or local beta-adrenergic agonist application.[20] Random DAD latency was simulated by randomly setting the SR Ca release time, and the amplitude of DAD was changed by varying the strength of the SR Ca release flux. The effects of Na channel availability, gap junction coupling, as well as other factors, were characterized.

Methods

Simulations were performed in 1D cable and 2D tissue models. The partial differential equation governing voltage is:

$$\frac{\partial V}{\partial t} = -I_{ion}/C_m + D\left(\frac{\partial^2 V}{\partial x^2} + \frac{\partial^2 V}{\partial y^2}\right) \quad (1)$$

where V is membrane voltage; $C_m = 1$ μF/cm^2 is membrane capacitance, and D is the diffusion constant (proportional to gap junction conductance) with its control value set as 0.0005 cm^2/ms. The AP model and generation of DADs were described previously by Xie et al.[21] The spontaneous SR Ca release strength is described by a parameter g_{spon}, and the random latency of the release follows a gaussian distribution of standard deviation σ. More details of the model and simulation methods given in the Online Supplemental Material.

In the simulations, unless specified the maximum Na channel conductance (g_{Na}) was 12 pA/pF and the Na channel steady-state inactivation curve (h_∞) was left-shifted 5 mV (ie, $V_{1/2}$ was changed from –66 to –71 mV). Figure 1A shows example traces of DADs and TA for different g_{spon} values. Figure 1B shows the maximum voltage vs g_{spon}. The threshold for suprathreshold DADs or TA in a single cell was $g_{spon} = 0.066$ ms^{-1} (arrow in Figure 1B) without the shift of h_∞, but with a 5-mV left-shift, it increased to 0.0695 ms^{-1}.

Results

Effects of subthreshold DADs

Subthreshold DADs can cause conduction block when Na channel availability is reduced

We simulated a 1D cable in which the middle third of the cells exhibited DADs (Figure 2). We assumed that the spontaneous Ca releases causing DADs were identical and occurred at the same time in each cell (Figure 2A). A premature stimulus was applied to the first 10 cells at the end of the cable, and the ability of the AP to propagate to the other end of the cable was studied for different DAD amplitudes (adjusted by varying g_{spon}) and coupling intervals. For normal Na channel properties in our model, subthreshold

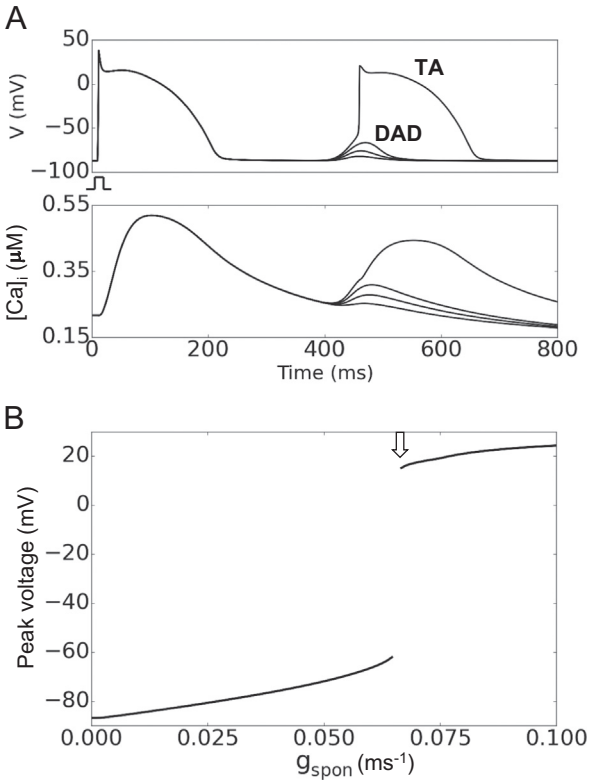

Figure 1 The delayed afterdepolarization (DAD) model. **A:** DADs and triggered activity (TA) from a single isolated cell for different g_{spon} values. *Top traces* show membrane potential. *Bottom traces* show the corresponding intracellular Ca concentrations. **B:** Maximum DAD voltage amplitude vs g_{spon}. *Arrow* indicates g_{spon} threshold for a suprathreshold DAD eliciting TA.

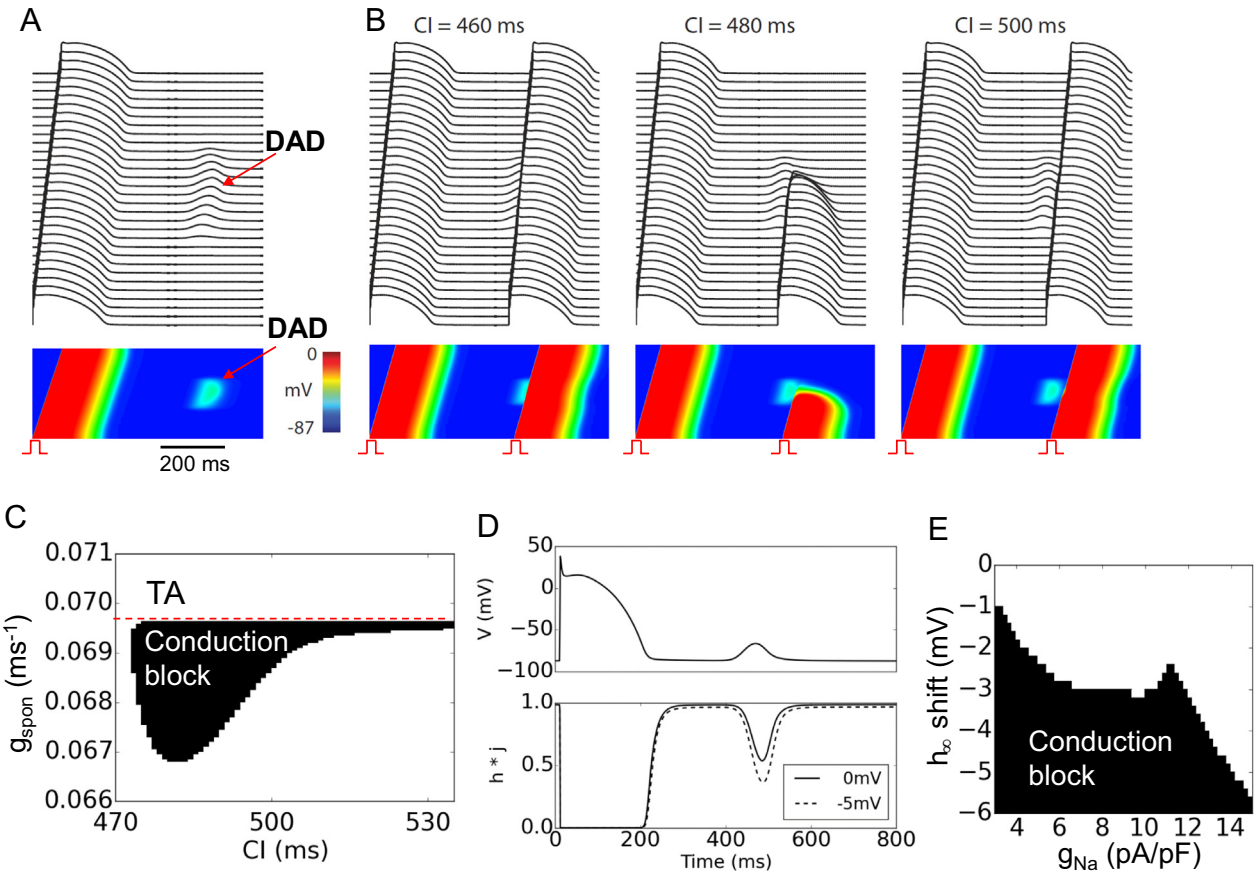

Figure 2 Conduction block due to a subthreshold delayed afterdepolarization (DAD) in a 1-dimensional cable. **A:** A 300-cell cable is paced at a cycle length of 500 ms and a subthreshold DAD occurs in the middle 100 cells approximately 450 ms after the action potential (AP) upstroke. *Top traces* show membrane potential of every 10th cell. *Bottom trace* shows a space–time plot of voltage along the cable. **B:** Under the same conditions, a premature stimulus elicited an AP (premature ventricular contraction [PVC]), which propagated into the DAD region. When the coupling interval (CI) of the PVC was 460 ms **(left)** or 500 ms **(right),** the PVC propagated successfully to the other end of the cable. For CI of 480 ms **(middle),** however, conduction block occurred in the DAD region. **C:** A parameter diagram showing conduction block (in *black*) as a function of CI and g_{spon}. *Dashed line* indicates the transition from a subthreshold to suprathreshold DAD causing triggered activity (TA) at $g_{spon} = 0.0695\ ms^{-1}$. **D:** Voltage and Na channel availability (h*j) vs time for the unshifted *(solid)* and 5-mV left-shifted *(dashed)* h_∞ during a DAD. **E:** Conduction block as a function of g_{Na} and left-shift of h_∞.

DADs failed to cause conduction block, regardless of DAD amplitude or coupling interval. However, if Na channel availability was reduced by shifting the half-maximal voltage of steady-state inactivation (described by h_∞) in the negative direction, as might occur physiologically with protein kinase A (PKA), protein kinase C, or Ca/calmodulin-dependent protein kinase II (CaMKII) phosphorylation of Na channels[22] or in some Brugada syndrome mutations,[23] conduction block occurred over a range of coupling intervals when DAD amplitude reached a critical range (Figures 2B and 2C). In this range, DAD-induced depolarization caused sufficient Na channel inactivation, to result in conduction failure. Figure 2D illustrates the time course of Na channel availability (h*j) during a DAD with a peak voltage around –70 mV for control (solid) and for a 5-mV left-shift of h_∞ (dashed), showing that a 5-mV left-shift causes a large reduction in Na channel availability during the DAD. As the DAD amplitude was increased further ($g_{spon} > 0.0695\ ms^{-1}$), TA occurred in the DAD region, which propagated in both directions and collided retrogradely with the premature beat. Figure 2E plots the region of conduction block vs the left-shift of h_∞ and g_{Na}, showing that reducing g_{Na} also promoted conduction block.

Effects of random DAD latency

In the simulations shown in Figure 2, the spontaneous Ca releases causing a DAD in the midregion of the cable all occurred synchronously by design. To study the effects of random DAD latency, we simulated a 1D cable in which the latency of the spontaneous Ca release event for each cell was randomly assigned from a gaussian distribution. Gap junction coupling naturally smoothed the resulting DAD in the tissue (Figure 3A). Unlike the nonrandom case shown in Figure 2, a premature beat with a fixed coupling interval could either block or propagate successfully through the DAD region, depending on the particular randomization pattern of the trial (Figure 3B). The probability of conduction failure through the DAD region vs the strength of spontaneous Ca release (g_{spon}) for different standard deviations (σ) of the gaussian distribution of latencies, g_{Na}, and gap junction coupling are shown in Figures 3C–3E. Increasing σ caused conduction block to occur over a broader range of

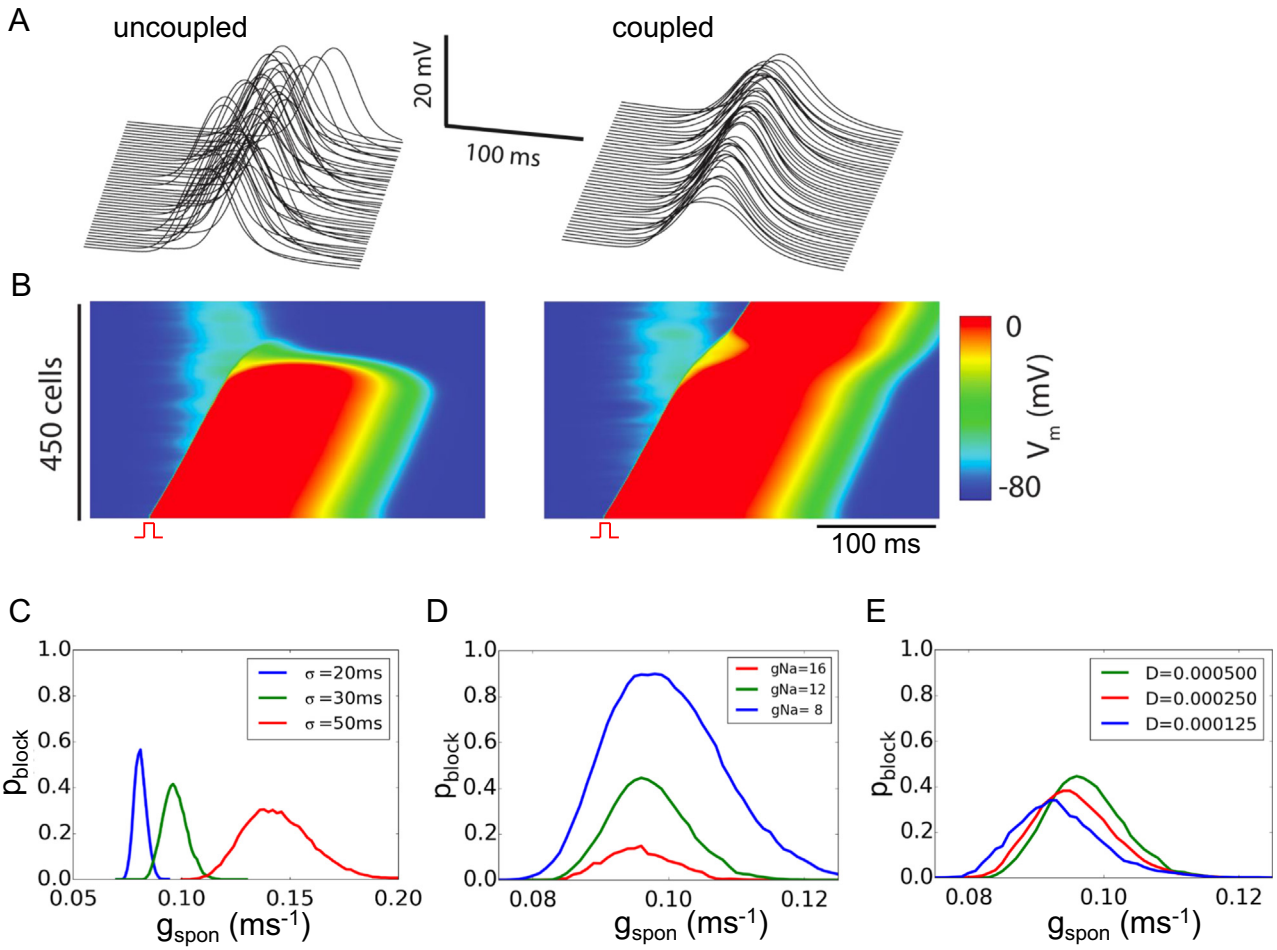

Figure 3 Effects of delayed afterdepolarization (DAD) synchronization on conduction block. **A:** Random DAD latency when the cells in a 1-dimensional cable are electrically uncoupled **(left)** or coupled by gap junctions **(right),** illustrating the synchronizing effect of coupling on the tissue DAD. **B:** Voltage snapshots showing 2 different trials in which DAD latencies were randomly selected from a gaussian distribution with a standard deviation (σ) of 20 ms. The resulting subthreshold tissue DADs were sufficiently different to cause an identically timed premature ventricular contraction (PVC) to block in 1 trial **(left)** but successfully propagate in the other trial **(right). C–E:** Probability of conduction block (p_{block}) vs g_{spon} for different σ **(C),** g_{Na} **(D),** and D **(E)** in a cable length of 450 cells. The probability of each parameter point was calculated from 1000 random trials. The *green curve* in C–E is the control case with σ = 30 ms, D = 0.0005 cm^2/ms, g_{Na} = 12 pA/pF, and a –5 mV shift of h_∞.

g_{spon}. Note that in the nonrandom case, TA occurred when $g_{spon} > 0.0695$ ms^{-1}, and no conduction block occurred. With random latency, a higher g_{spon} was required to trigger APs because of the source–sink effects, and conduction block still occurred when $g_{spon} > 0.0695$ ms^{-1}. Reducing g_{Na} increased the probability of conduction block, whereas reducing gap junction coupling had a small effect.

If we applied the same deterministic or random DAD distribution as in the 1D cables (Figures 2 and 3) to 2D tissue, reentry could be induced by a premature stimulus (see Online Supplemental Videos 1 and 2).

Combined effects of suprathreshold and subthreshold DADs

In the simulations shown in Figure 2, external paced premature stimuli were used to illustrate how DADs can cause conduction block. We next examined whether TA self-generated by DADs could develop conduction block in the same cable due to random latency of DADs in different regions causing both subthreshold and suprathreshold DADs.

Complex excitation patterns in 1D cable

We performed simulations in a homogeneous 1D cable with random DAD latency as shown in Figure 3 without externally paced premature stimuli. Complex excitation patterns occurred, which could be classified into 3 categories: (1) subthreshold DADs without TA ((Figure 4A); 2) suprathreshold DADs causing TA, which propagated successfully along the cable without conduction block (Figure 4B); and (3) suprathreshold DADs causing TA, which propagated partway before developing conduction block (Figure 4C). Figure 4D shows the probability of the 3 behaviors as a function of DAD amplitude (g_{spon}). No TA occurred when g_{spon} was small, but as g_{spon} increased the incidence of TA also increased (dashed in Figure 4D). Due to random latency and cell coupling, the g_{spon} threshold for TA

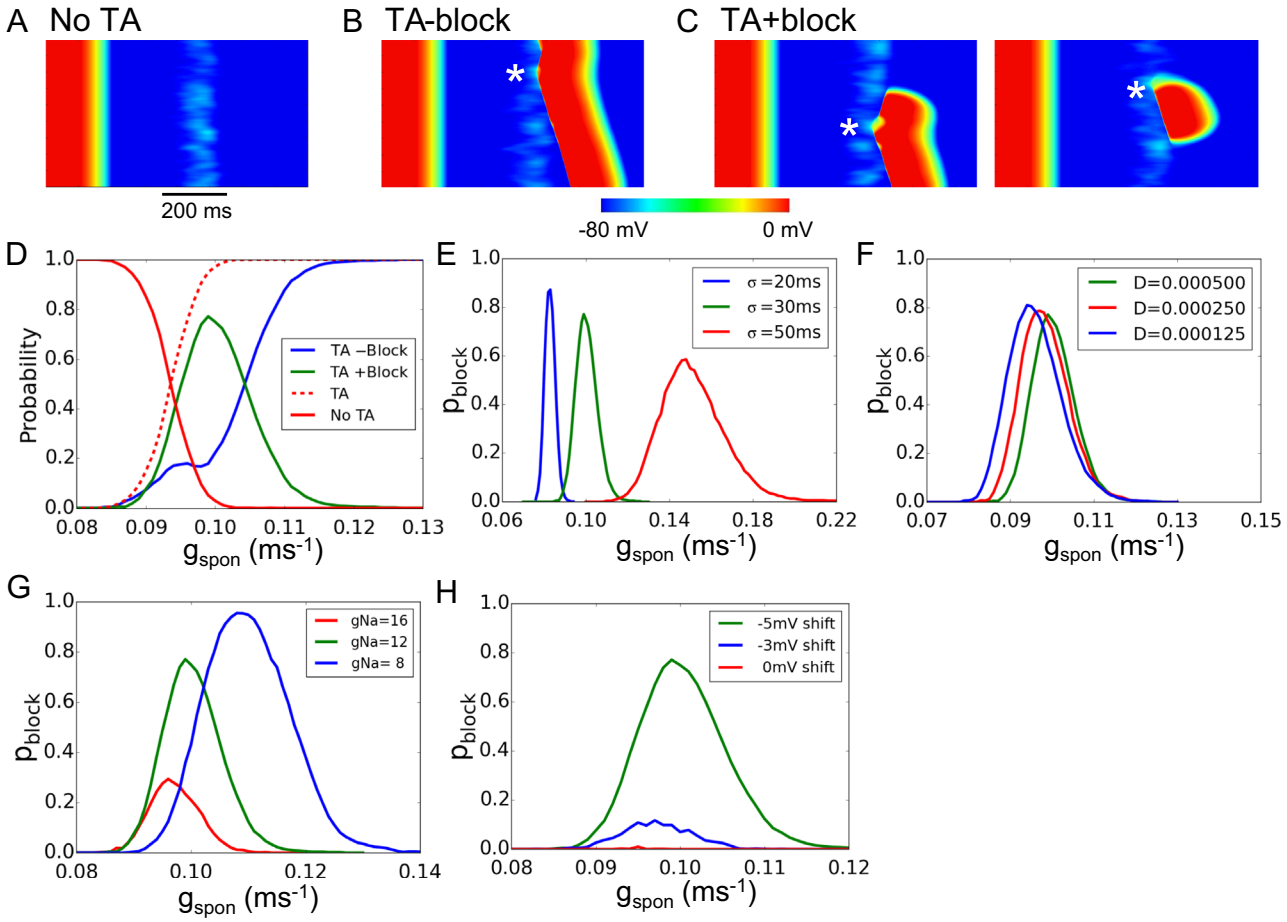

Figure 4 Complex excitation patterns in a 1-dimensional cable. **A–C:** Space–time plots of membrane potential vs time in a 300-cell cable in which all cells exhibited delayed afterdepolarizations (DADs) with randomly assigned latencies ($\sigma = 50$ ms) following a paced action potential. $g_{spon} = 0.15$ ms^{-1}. Asterisk in B and C indicates the earliest site of TA. **D:** Probability of no triggered activity (TA; *red*), a successfully propagating TA *(blue)*, and a TA with conduction block *(green)* vs g_{spon} for $\sigma = 30$ ms. **E:** Probability of conduction block vs g_{spon} for different σ. **F:** Probability of conduction block vs g_{spon} for different diffusion coefficients (D) reflecting gap junction coupling. **G:** Probability of conduction block vs g_{spon} for different g_{Na}. **H:** Probability of conduction block vs g_{spon} for shifts in the half-maximal voltage of h_∞. The cable length in D–H was 450 cells. The probability of each parameter point was calculated from 1000 random trials. The *green curve* in D–H is the control case with $\sigma = 30$ ms, $D = 0.0005$ cm^2/ms, $g_{Na} = 12$ pA/pF, and a –5 mV shift of h_∞.

was higher in tissue than in a single cell ($g_{spon} > 0.0695$ ms^{-1}). The probability of block increases with broadened latency distribution (Figure 4E), decreased cell coupling (Figure 4F), reduced g_{Na} (Figure 4G), and left-shifted h_∞ (Figure 4H).

Reentry initiation in 2D tissue

Unidirectional conduction block of DAD-mediated TA in the 1D cable raises the possibility that under similar conditions in 2D tissue, reentry may be induced when conduction block is appropriately localized. Analogous to the 1D simulations shown in Figures 3 and 4, we first simulated a homogeneous 2D tissue in which all cells were identical with the same DAD amplitude (ie, identical g_{spon}), but DAD latencies were randomly assigned following a gaussian distribution. Both subthreshold DADs and TA were observed, but in more than 10,000 simulations using different parameter settings, reentry was never observed, even when g_{Na} or gap junction coupling was reduced.

Because Ca release properties in real cardiac tissue are not homogeneous, we then performed simulations in which g_{spon} was varied in random checkerboard patterns, drawing from a gaussian distribution (Figure 5A). Checker sizes ranged from 1×1 to 256×256 cells. DAD latencies were still varied randomly from cell to cell as in the simulations described earlier. We observed 3 behaviors (Figure 5B): (1) all DADs are subthreshold (no TA); (2) DADs induce TA without reentry formation (TA without reentry); and (3) DADs induce TA with reentry formation (TA with reentry). Figure 5C shows the probability of these different behaviors vs the checker size for control parameters. For large checker sizes, the majority of the simulations exhibited TA without reentry (ie, PVCs only), and a small number of the simulations exhibited reentry. As the checker size decreased, the probability of TA without reentry decreased, whereas that of subthreshold DADs increased. Interestingly, the probability of reentry first increased and then decreased to zero at small checker sizes. Reducing gap junction conductance selectively increased the probability of reentry at large and small checker sizes (Figure 5D) but suppressed reentry at intermediate checker sizes. Reducing Na channel

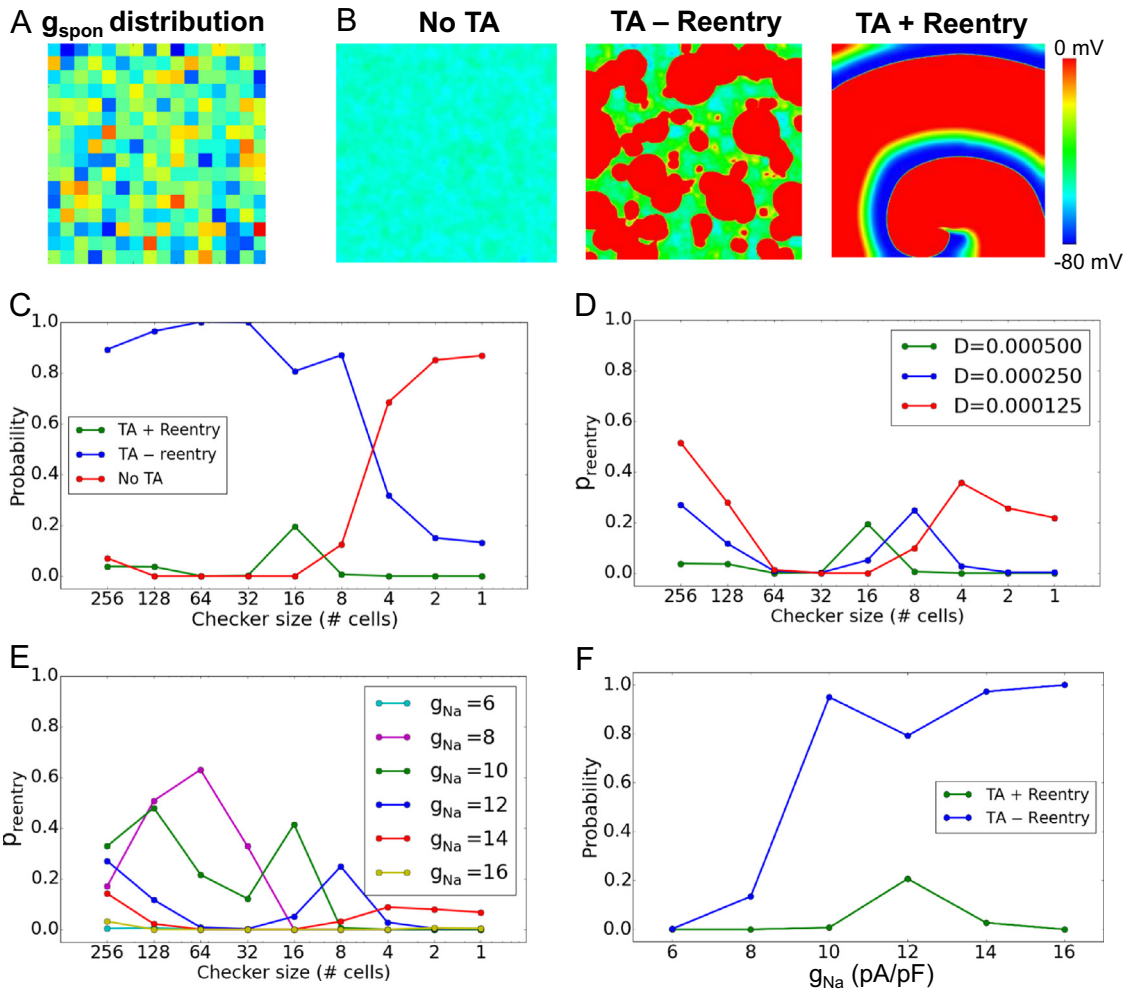

Figure 5 Summary data for reentry induction in heterogeneous 2-dimensional tissue. **A:** Example of checkerboard g_{spon} distribution. g_{spon} in each checker was drawn from a random gaussian distribution with an average value of 0.172 ms^{-1} and a standard deviation $\sigma = 0.03$ ms^{-1}. **B:** Examples of voltage snapshots illustrating no triggered activity (TA), TA – reentry, and TA + reentry. **C:** Probability of TA + reentry *(green)*, TA – reentry *(blue)*, and no TA *(red)* vs checker size. *Dashed line* indicates the total probability of TA. **D:** Probability of reentry vs checker size for different diffusion coefficients (D, cm^2/ms). **E:** Probability of reentry for different g_{Na}. **F:** Probability of TA – reentry and TA + reentry vs g_{Na} for an 8×8 checker size. The standard deviation for random delayed afterdepolarization (DAD) latency of individual cells was $\sigma = 50$ ms. Tissue size was 512×512 cells. The probability of each parameter point was calculated from 500 random trials.

conductance g_{Na} in steps from 16 to 8 pS/pF increased the probability of reentry, particularly at large checker sizes, whereas further reduction to 6 pS/pF suppressed reentry due to low excitability (Figure 5E). Figure 5F compares the probability of TA with and without reentry vs g_{Na}. As g_{Na} was reduced, the probability of TA without reentry decreased, whereas the probability of TA with reentry first increased then decreased. We also performed simulations in which g_{spon} was varied randomly in checkerboard patterns, but DAD latency was fixed. We never observed reentry, indicating that the random DAD latency is a key property promoting reentry. This was also supported by simulations investigating the effect of DAD latency distribution on reentry in 2D tissue, which depended sensitively on σ (see Online Supplementary Figure 1).

Finally, we examined how electrical remodeling in heart failure affects DAD-mediated arrhythmogenesis (Figure 6). Electrical remodeling decreased the threshold of g_{spon} required for conduction block (Figure 6A) and greatly decreased the g_{spon} required for TA with reentry (Figure 6B). Similar to Figure 5F, decreasing g_{Na} reduced the probability of TA without reentry and first increased then decreased the probability of TA with reentry (Figure 6C).

Checker size had a nonmonotonic effect on probability of reentry (Figures 5 and 6). A possible explanation is illustrated in Figure 7, which shows voltage snapshots for 3 different checker sizes with reduced gap junction coupling. For the 256×256 case (Figure 7A and Online Supplemental Video 3), the randomness of DAD latency resulted in nonuniform DAD voltages in a single checker, allowing conduction in 1 direction but block in another direction at the borders of the individual checkers. Because of the large checker size, there was enough room for the broken wavefronts to turn and reenter the checker from another direction. For the 32×32 case (Figure 7B and Online Supplemental Video 4), TA that formed in the individual checkers tended

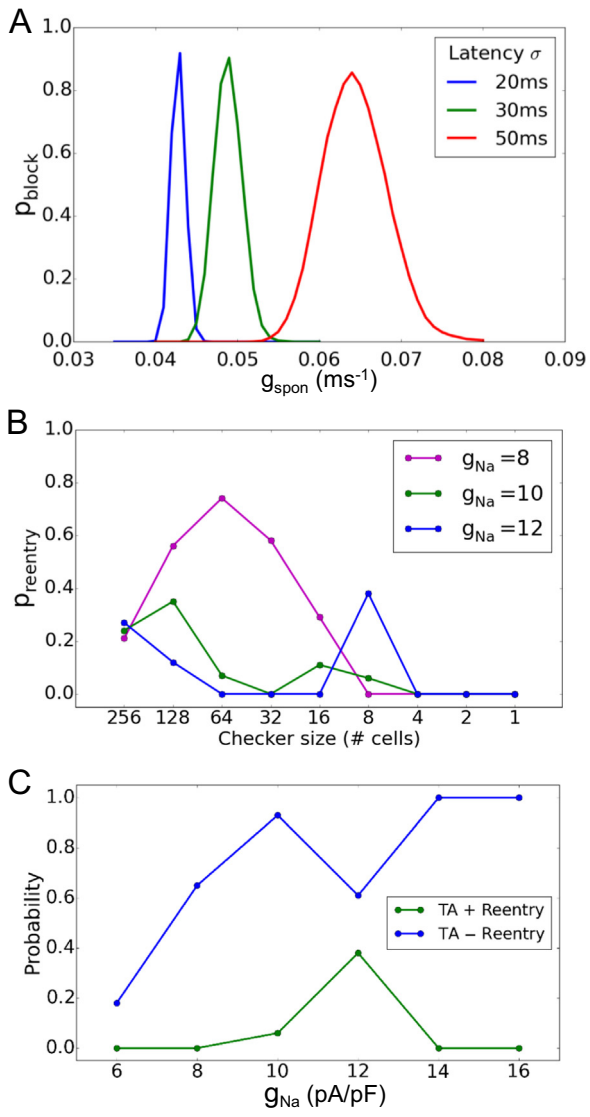

Figure 6 Conduction block and reentry in heart failure. Heart failure was simulated as described in Xie et al.[21] **A:** Probability of conduction block in a 1-dimensional cable vs g_{spon} for different delayed afterdepolarization (DAD) latency σ. The g_{spon} range for conduction block is lower than in the nonfailing condition (Figure 4E). **B**: Probability of triggered activity (TA) + reentry (green) vs checker size in a 2-dimensional tissue of failing cells for different g_{Na}. g_{spon} was drawn from a gaussian distribution with an average value of 0.065 ms^{-1} and a standard deviation of $\sigma = 0.02$ ms^{-1}. DAD latency standard deviation $\sigma = 50$ ms. **C:** Probability of TA – reentry and TA + reentry vs g_{Na}.

to propagate neatly in all directions and fuse together, such that there was not enough unexcited tissue for a broken wavefront to form a spiral wave. For the 1×1 case (Figure 7C and Online Supplemental Video 5), the checkers with high g_{spon} values were not large enough to generate TA individually unless neighboring checkers also had randomly been assigned large enough g_{spon} values to overcome the source–sink mismatch. This effectively resulted in large heterogeneous regions with or without TA, increasing the probability of reentry. Note that when the gap junction coupling was normal, however, no reentry could occur for the 1×1 case (Figure 5C).

Discussion

DADs are classically recognized as triggers of PVCs that can initiate reentry when they encounter a vulnerable tissue substrate. In this study we demonstrate that subthreshold DADs can also directly generate a tissue substrate vulnerable to unidirectional conduction block. Moreover, DAD-induced triggers and substrates can occur simultaneously in the same tissue to induce reentry. These effects are enhanced with reduced Na channel availability and gap junction coupling, with electrical remodeling changes in heart failure, and when regional differences in Ca cycling properties underlying DADs are accentuated, as occurs in the setting of heart diseases. Thus, our observations provide novel insights into DAD-related arrhythmogenesis.

Roles of DADs in cardiac arrhythmogenesis

Based on observations in the present study, we can summarize the roles of DADs in cardiac arrhythmogenesis as follows.

DADs generate arrhythmia triggers

The well-known effect of suprathreshold DADs in cardiac arrhythmogenesis is their ability to trigger an AP and generate TA, which can cause focal (nonreentrant) arrhythmias or serve as PVCs to initiate reentrant arrhythmias.[1–3,24,25]

DADs generate a vulnerable substrate

Traditionally, dispersion of excitability and/or refractoriness make a tissue vulnerable to initiation of reentry by a trigger such as a PVC.[26] Unidirectional conduction block initiating reentry occurs because either the Na current has not recovered sufficiently from inactivation to overcome the source–sink mismatch of neighboring repolarized cells (dispersion of excitability) or the neighboring cells are still in a refractory state (dispersion of refractoriness). In this study, we demonstrated that subthreshold DADs can cause unidirectional conduction block via the former mechanism by elevating diastolic membrane potential and inactivating Na channels sufficiently to cause conduction block. The random distribution of DAD latency increases the probability of conduction block (Figure 3) because as DAD latency distribution becomes wider, DAD duration in the tissue prolongs, giving more time for more Na channels to inactivate.

Because subthreshold DADs can occur at any time during diastole, a very late diastolic subthreshold DAD could potentially cause regional conduction block of a subsequent sinus beat, initiating reentry directly from sinus rhythm in the absence of a PVC. In this case, the first beat of reentrant ventricular tachycardia would have the same QRS morphology as subsequent tachycardia beats, which is frequently observed in clinical studies.[27] Thus, unlike reentrant arrhythmias induced by dispersion of refractoriness in which an external PVC usually is required, DAD-mediated reentrant arrhythmias do not necessarily require an external PVC, as the next sinus beat can serve to initiate reentry.

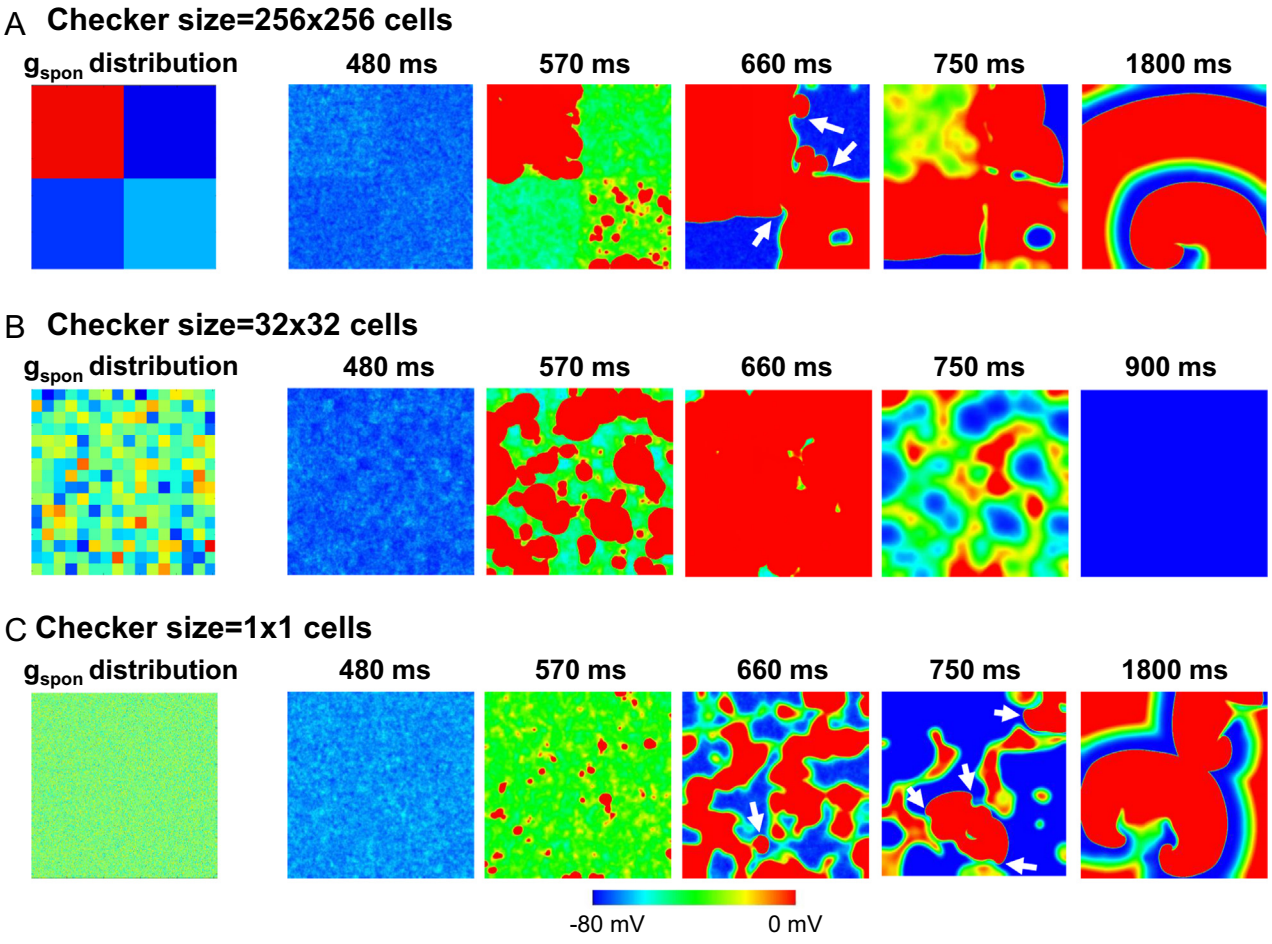

Figure 7 Voltage snapshots for 3 different checker sizes in heterogeneous 2-dimensional tissue. **Left panels** show g_{spon} distributions and **right panels** show corresponding voltage snapshots of delayed afterdepolarization (DAD)-mediated triggered activity (TA) and conduction block at various times after a paced action potential, with checker sizes of 256×256 **(A),** 32×32 **(B),** and 1×1 **(C)** cells.

DADs simultaneously generate triggers and a vulnerable substrate

Because of random[5,16,17] and heterogeneous[3,18] Ca release, DADs in tissue can lead to complex depolarization patterns in which some regions generate suprathreshold DADs causing TA, whereas other regions generate subthreshold DADs promoting regional conduction block and initiation of reentry (Figures 4–7). TA generated in 1 region may propagate in all or in only 1 direction, or may be blocked a distance away such that reentry can result if the broken wavefronts have enough available excitable tissue. Although the interactions among random latency, heterogeneity, gap junction coupling, and Na channel availability are complex, the probability of conduction block and reentry increases for reduced gap junction coupling, Na current availability, and electrical remodeling. Our simulations also show that both random latency and heterogeneous Ca release are needed for reentry to occur.

Clinical significance

As shown in our simulations (Figures 4–6), a negative shift in the steady-state inactivation curve and/or reduction of the maximal Na conductance increased the probability of conduction block and reentry in the presence of DADs. This condition is physiologically mimicked by PKA- and/or PKC-mediated phosphorylation of Na channels during sympathetic stimulation or CaMKII-mediated phosphorylation of Na channels in the setting of heart failure,[22] Na channel remodeling in ischemic heart disease,[28] or loss-of-function Na channel mutations in Brugada syndrome[23] and other diseases.[29]

Because class I antiarrhythmic agents not only reduce the Na channel open probability but also left-shift the steady-state inactivation curve,[30] this may have been a contributing factor to the proarrhythmic effects of Na channel blockers observed in the Cardiac Arrhythmia Suppression Trial (CAST).[31] In CAST, Na channel blockers effectively suppressed PVCs by more than 80%, but mortality nevertheless increased due to more frequent lethal arrhythmic events. Many later studies established that blocking the Na channel is proarrhythmic in ischemic and infarcted tissue due to lowered excitability and increased postrepolarization refractoriness in the border zone.[28,30] Our simulations suggest that an additional mechanism could also be important: if the PVCs in these patients originated from Ca wave-mediated

DADs, then reducing excitability by blocking Na channels could have reduced the frequency of benign PVCs by converting suprathreshold DADs to subthreshold DADs, while at the same time paradoxically increasing the probability that the less frequent remaining suprathreshold DADs will initiate reentry. This phenomenon is illustrated in Figures 5F and 6C, in which reducing Na channel conductance reduced the incidence of TA without reentry (benign PVCs) but increased the probability of TA with reentry (malignant PVCs initiating ventricular tachycardia/ventricular fibrillation) over a certain range of g_{Na}.

Finally, PVCs can originate from either the His–Purkinje system or ventricular myocardium in patients, and they may exhibit simple patterns in the ECG, such as fixed QRS morphology (unifocal PVCs) and fixed coupling interval, or complex patterns such as different QRS morphologies (multifocal PVCs) and varying coupling intervals (modulated parasystole). For the mechanisms described in this study, we can speculate that PVCs arising from an abnormal area in the His–Purkinje system would tend to produce unifocal PVCs with some degree of variation in coupling intervals. In ventricular tissue, on the other hand, the random process by which Ca waves in individual myocytes self-organize to generate suprathreshold vs subthreshold DADs in different regions of tissue would likely produce multifocal PVCs with variable coupling intervals. Another potential insight from the current study relates to the hypothesis that subthreshold DADs occurring in ventricles may be one of the mechanisms underlying U waves in the ECG,[32] as supported by recent experimental studies.[13] Based on our finding that subthreshold DADs also can create a vulnerable substrate for reentry, it is intriguing to speculate that PVCs accompanying U waves in the ECG may confer a higher arrhythmia risk than when U waves are absent.

Study limitations

A limitation of this study is that the DADs in our model were caused by commanded SR Ca releases with randomly distributed amplitude and/or latency following gaussian distributions, which allowed us to readily control DAD amplitude and latency. To realistically simulate spontaneous Ca release via the mechanism of Ca-induced Ca release and the feedback between Ca and voltage requires a detailed Ca cycling model incorporating random ryanodine receptor openings.[5,33,34] We studied only the effects of voltage depolarization on conduction block and not the feedback between Ca and voltage or other excitation–contraction dynamics, but the simulation results from the present study still provide important mechanistic insights into arrhythmias caused by DADs. We altered DAD amplitude by increasing spontaneous SR Ca release, but DAD amplitude also can be regulated by the diastolic Ca-voltage coupling gain,[35] which we did not study except in the context of heart failure electrical remodeling (Figure 6). We also did not explicitly study the effects of altering DAD duration at the cellular level, which in real cells is sensitive to the subcellular location and numbers of sites from which Ca waves originate. Our 1D and 2D tissue models are relatively simple compared to real tissue, and the results may be influenced by specific structural features of the tissue. For example, as shown in Figure 5, the proarrhythmic effects of blocking Na channels or reducing gap junction conductance depended on the specific spatial characteristics of heterogeneities. Nevertheless, the insights from computer modeling in this study have uncovered novel mechanisms for DAD-mediated arrhythmogenesis that provide testable hypotheses for future experimental studies.

Conclusion

Whereas suprathreshold DADs in cardiac tissue generate triggers for reentrant arrhythmias, subthreshold DADs can create regions susceptible to unidirectional conduction block, directly increasing the probability that the triggers will induce reentry. This scenario is unlikely when Na channel properties are normal but becomes increasingly probable as Na channel availability is reduced by sympathetic stimulation, disease-related remodeling, loss-of-function genetic defects, or class I antiarrhythmic drugs, and as gap junction coupling is reduced by gap junction remodeling or fibrosis. These dynamics provide novel mechanistic insights into DAD-mediated arrhythmogenesis potentially relevant to a spectrum of cardiac diseases such as chronic ischemia, heart failure, Brugada syndrome, and catecholaminergic polymorphic ventricular tachycardia, as well as the proarrhythmic effects of Na channel blockers.

Appendix

Supplementary data

Supplementary material cited in this article is available online at http://dx.doi.org/10.1016/j.hrthm.2015.06.019.

References

1. Rosen MR, Moak JP, Damiano B. The clinical relevance of afterdepolarizations. Ann N Y Acad Sci 1984;427:84–93.
2. January CT, Fozzard HA. Delayed afterdepolarizations in heart muscle: mechanisms and relevance. Pharmacol Rev 1988;40:219–227.
3. Katra RP, Laurita KR. Cellular mechanism of calcium-mediated triggered activity in the heart. Circ Res 2005;96:535–542.
4. Cheng H, Lederer MR, Lederer WJ, Cannell MB. Calcium sparks and [Ca^{2+}]i waves in cardiac myocytes. Am J Physiol 1996;270:C148–C159.
5. Nivala M, Ko CY, Nivala M, Weiss JN, Qu Z. Criticality in intracellular calcium signaling in cardiac myocytes. Biophys J 2012;102:2433–2442.
6. Yeh YH, Wakili R, Qi XY, et al. Calcium-handling abnormalities underlying atrial arrhythmogenesis and contractile dysfunction in dogs with congestive heart failure. Circ Arrhythm Electrophysiol 2008;1:93–102.
7. Pogwizd SM, Bers DM. Calcium cycling in heart failure: the arrhythmia connection. J Cardiovasc Electrophysiol 2002;13:88–91.
8. Hoeker GS, Katra RP, Wilson LD, Plummer BN, Laurita KR. Spontaneous calcium release in tissue from the failing canine heart. Am J Physiol Heart Circ Physiol 2009;297:H1235–H1242.
9. Ross JL, Howlett SE. ß-adrenoceptor stimulation exacerbates detrimental effects of ischemia and reperfusion in isolated guinea pig ventricular myocytes. Eur J Pharmacol 2009;602:364–372.
10. Watanabe H, Chopra N, Laver D, et al. Flecainide prevents catecholaminergic polymorphic ventricular tachycardia in mice and humans. Nat Med 2009;15:380–383.
11. Mohler PJ, Schott J-J, Gramolini AO, et al. Ankyrin-B mutation causes type 4 long-QT cardiac arrhythmia and sudden cardiac death. Nature 2003;421:634–639.

12. Burashnikov A, Antzelevitch C. Acceleration-induced action potential prolongation and early afterdepolarizations. J Cardiovasc Electrophysiol 1998;9:934–948.
13. Morita H, Zipes DP, Morita ST, Wu J. Mechanism of U wave and polymorphic ventricular tachycardia in a canine tissue model of Andersen-Tawil syndrome. Cardiovasc Res 2007;75:510–518.
14. Singer DH, Lazzara R, Hoffman BF. Interrelationship between automaticity and conduction in Purkinje fibers. Circ Res 1967;21:537–558.
15. Rosen MR, Wit AL, Hoffman BF. Electrophysiology and pharmacology of cardiac arrhythmias. IV. Cardiac antiarrhythmic and toxic effects of digitalis. Am Heart J 1975;89:391–399.
16. Wasserstrom JA, Shiferaw Y, Chen W, et al. Variability in timing of spontaneous calcium release in the intact rat heart is determined by the time course of sarcoplasmic reticulum calcium load. Circ Res 2010;107:1117–1126.
17. Fujiwara K, Tanaka H, Mani H, Nakagami T, Takamatsu T. Burst emergence of intracellular Ca^{2+} waves evokes arrhythmogenic oscillatory depolarization via the Na^{+}-Ca^{2+} exchanger: simultaneous confocal recording of membrane potential and intracellular Ca^{2+} in the heart. Circ Res 2008;103:509–518.
18. Plummer BN, Cutler MJ, Wan X, Laurita KR. Spontaneous calcium oscillations during diastole in the whole heart: the influence of ryanodine reception function and gap junction coupling. Am J Physiol Heart Circ Physiol 2011;300:H1822–H1828.
19. Schlotthauer K, Bers DM. Sarcoplasmic reticulum Ca(2+) release causes myocyte depolarization. Underlying mechanism and threshold for triggered action potentials. Circ Res 2000;87:774–780.
20. Myles RC, Wang L, Kang C, Bers DM, Ripplinger CM. Local β-adrenergic stimulation overcomes source-sink mismatch to generate focal arrhythmia. Circ Res 2012;110:1454–1464.
21. Xie Y, Sato D, Garfinkel A, Qu Z, Weiss JN. So little source, so much sink: requirements for afterdepolarizations to propagate in tissue. Biophys J 2010;99:1408–1415.
22. Herren AW, Bers DM, Grandi E. Post-translational modifications of the cardiac Na channel: contribution of CaMKII-dependent phosphorylation to acquired arrhythmias. Am J Physiol Heart Circ Physiol 2013;305:H431–H445.
23. Hu D, Barajas-Martinez H, Burashnikov E, et al. A mutation in the β3 subunit of the cardiac sodium channel associated with Brugada ECG phenotype. Circ Cardiovasc Genet 2009;2:270–278.
24. Pogwizd SM, Bers DM. Cellular basis of triggered arrhythmias in heart failure. Trends Cardiovasc Med 2004;14:6166.
25. Rubart M, Zipes DP. Mechanisms of sudden cardiac death. J Clin Invest 2005;115:2305–2315.
26. Qu Z, Weiss JN. Mechanisms of ventricular arrhythmias: from molecular fluctuations to electrical turbulence. Annu Rev Physiol 2015;77:29–55.
27. Saeed M, Link MS, Mahapatra S, et al. Analysis of intracardiac electrograms showing monomorphic ventricular tachycardia in patients with implantable cardioverter-defibrillators. Am J Cardiol 2000;85:580–587.
28. Pu J, Boyden PA. Alterations of Na+ currents in myocytes from epicardial border zone of the infarct heart: a possible ionic mechanism for reduced excitability and postrepolarization refractoriness. Circ Res 1997;81:110–119.
29. Grant AO, Carboni MP, Neplioueva V, et al. Long QT syndrome, Brugada syndrome, and conduction system disease are linked to a single sodium channel mutation. J Clin Invest 2002;110:1201–1209.
30. Pu JL, Balser JR, Boyden PA. Lidocaine action on Na^{+} currents in ventricular myocytes from the epicardial border zone of the infarcted heart. Circ Res 1998;83:431–440.
31. Echt DS, Liebson PR, Mitchell LB, et al. Mortality and morbidity in patients receiving encainide, flecainide, or placebo. The Cardiac Arrhythmia Suppression Trial. N Engl J Med 1991;324:781–788.
32. Surawicz B. U wave: facts, hypotheses, misconceptions, and misnomers. J Cardiovasc Electrophysiol 1998;9:1117–1128.
33. Chen W, Asfaw M, Shiferaw Y. The statistics of calcium-mediated focal excitations on a one-dimensional cable. Biophys J 2012;102:461–471.
34. Song Z, Ko Christopher Y, Nivala M, Weiss James N, Qu Z. Calcium-voltage coupling in the genesis of early and delayed afterdepolarizations in cardiac myocytes. Biophys J 2015;108:1908–1921.
35. Maruyama M, Joung B, Tang L, et al. Diastolic intracellular calcium-membrane voltage coupling gain and postshock arrhythmias: role of Purkinje fibers and triggered activity. Circ Res 2010;106:399–408.

CLINICAL PERSPECTIVES

Delayed afterdepolarizations (DADs) are well known as arrhythmia triggers, but their role in creating a vulnerable tissue substrate for reentry has not been comprehensively investigated. In this study, we showed that DADs that do not reach threshold for triggered activity can create a vulnerable tissue substrate by regionally decreasing excitability sufficiently to cause conduction block. Moreover, when both subthreshold and suprathreshold DADs coexist in the same tissue, the combination of triggers and a vulnerable substrate can lead directly to reentry initiation. These effects are enhanced when sodium (Na) channel availability and gap junction coupling are reduced and tissue heterogeneities are enhanced, as occurs in the setting of heart disease. Because reduced Na channel availability potentiates this mechanism, Na channel blocking drugs may also be proarrhythmic by this mechanism.